Eurographics/ IEEE-VGTC Symposium on Visualization (2006)
Thomas Ertl, Ken Joy, and Beatriz Santos (Editors)

Segmentation of Flow Fields using Pattern Matching

J. Ebling [1] and G. Scheuermann [1]

[1]Universität Leipzig, Germany

Abstract

Due to the amount of data nowadays, automatic detection, classification and visualization of features is necessary for a thorough inspection of flow data sets. Pattern matching using vector valued templates has already been applied successfully for the detection of features. In this paper, the approach is extended to automatically compute feature based segmentations of flow data sets. Different problems of the segmentation like the influence of thresholds, overlapping features, and classification errors are discussed. Visualizations of the segmentation display important structures of the flow and highlight the interesting features. The segmentation algorithm presented in this paper is applicable to 2D and 3D vector fields as well as to time-dependent data.

Categories and Subject Descriptors (according to ACM CCS): I.4.6 [Computing Methodologies]: Image Processing and Computer VisionSegmentation; J.2 [Computer Applications]: Physical Sciences and Engineering

1. Introduction

A huge amount of data is generated nowadays by flow simulations and measurements. The resulting vector fields often contain millions of data values, but even for small datasets with only thousands of values, direct inspection by the user is tedious and features are missed easily. Therefore, many automated feature detection methods have been developed in the last years (e.g. [ES03, HEWK03, KHL99, Rot00], an overview can be found in [PVH*03]). However, often only one feature class is visualized afterwards. On the other hand, there are some overall visualizations like Line Integral Convolution (LIC) [CL93] and vector field topology [HH91]. LIC results in quite intuitive visualizations in 2D, but the features themselves are not emphasized and can still be missed. Visualization of vector field topology is a widely used technique in 2D though the topology may have to be simplified first [Tri02]. A successful adaptation of both approaches to 3D is hard due to the visibility problems in 3D, and has not been solved completely. Another, quite different, approach for the visualization is to use information visualization methods like brushing for interactive exploration of the data sets [DGH03].

Often, users ask specifically for a feature based segmentation of their data, that is, they want to know all features with their parameters like position, size, shape, radial velocity, etc. In contrast to image processing, features in vector fields are scarcely characterized by edges or borders. Therefore, segmentation based on edge information will not yield convincing results on flow fields. So far, segmentation of flow fields has been based mostly on topology [HH91] or clustering algorithms [GPR*04]. One feature based segmentation using anisotropic diffusion of LIC was developed in [DPR00].

In this paper, an algorithm for segmenting vector fields based on template matching is given. Pattern matching has already been proven useful for the detection and quantification of features in flow fields [ESvdW05]. Using template matching to compute a segmentation of flow fields has several advantages. First of all, the segmentation is based on the features themselves (Figure 2). Another advantage is that feature models used by engineers can be coded into the templates and thus automatic determination of the model parameters is possible within this framework as well. Furthermore, in some applications [vdWBY*04], the user is not interested as much in the actual flow behavior as in an approximation of the phenomena using simpler features models. Then, superposition effects have to be taken into account in order to analyze these features and compute their parameters, which is possible within this framework.

2. Related Work

Segmentation is well known from image processing [Jäh02, Jai89]. However, not all approaches can be transfered to flow fields due to the inherent properties of the features in the flow. In Section 2.1, an overview of the different techniques of segmenting an image is given along with a discussion of whether this approach is promising on flow fields, too. Existing segmentation approaches on vector fields are presented within this overview as well. An overview of template matching in vector fields, including the approach used in this paper, is described in Section 2.2.

2.1. Segmentation of Images

There are several approaches to segment an image. When the amplitude sufficiently characterizes the features, amplitude thresholding is useful. The results can afterwards be used for component labeling, where the connectivity of pixels with their neighbors is examined in order to assign the pixel to objects. In vector fields, the amplitude or velocity of the vector field usually does not code enough information for segmentation. On the other hand, amplitude thresholding of derived values like vorticity or similarity values from template matching can be quite useful for first analysis steps.

Another classical approach for segmentation in image processing is edge based. The edges of objects are combined to form boundaries, which then determine the objects. In vector fields, this might work for shock waves, shear flow, and convergent and divergent lines, as these can be interpreted as edges. However, segmentation should also classify these features. Furthermore, feature models of vortices, sinks, sources and saddles often have no real boundary, e.g. the Vatistas vortex [Vat98], a vortex model used by engineers. There, the vortex is assumed to be spread out infinitely though the influence of the vortex to the flow is nearly zero outside a certain region around the vortex center. The vortex core center is given by the maximum of the velocity profile, but the transition from inside the vortex core to the outside is usually smooth. This behavior is also typical for other flow features. Therefore, edge based segmentation in flow fields will not yield satisfactory results.

Looking at the vectors within a vortex or a swirling motion (e.g. Figure 6), it can be seen quite well that a vortex consist of velocities of all possible directions. Thus, it becomes quite clear that region based approaches and clustering [GPR*04], which group similar velocities, will not work for a feature centered segmentation of vector fields. Computing the topology of a vector field yields a segmentation of the flow into regions of same flow behavior. However, the features can not be classified or quantified well (Figure 2 and 6), and the problem of convincing 3D visualizations remains.

Segmentation based on anisotropic diffusion of LIC images [DPR00] results in a feature based segmentation. However, there is no criteria to stop the diffusion process, making the results not easily qualifiable. Furthermore, the problem of classification and quantification of the segmented features remains.

The Helmholtz-Hodge decomposition [PP00, PP03, TLHD03] separates a vector field into a divergent-free and a curl-free potential and a homogean part. Local extrema of the two potentials indicate sources, sinks, and swirling flows. The resulting vector fields can be used for further analysis of these features. However, other features like saddles are not included into this approach. Furthermore, features that are close to the boundary lead to significant changes in the structure of the whole field.

Pattern matching has been used for segmentation of images as well. There, similarity information of several different templates is computed at all pixels in the image, the features are classified according to the results and the image is then segmented into the regions of the features and background information. This approach is transfered to vector fields in this paper.

2.2. Pattern Matching on Vector Fields

An obvious approach to image processing of vector fields is to decompose the field into its components for subsequent independent processing using known tools such as convolution and the Fourier transform. Granlund and Knutson [GK95] have investigated this approach in 2D. However, the template matching should result in a rotation independent similarity measure, and thus this approach is not feasible.

Another definition of the convolution is the generalized inner product of pertinent vectors. Heiberg et al. [HEWK03] define convolution on vector fields using the inner (or scalar) product of two vectors as

$$(h *_S f)(x) = \int_{E^d} \langle h(x'), f(x-x') \rangle dx',$$

where f is the normalized vector field and h is the filter. The scalar product provides an approximation to the cosine of the angle between the direction of patterns present in the vector field and the direction of the filter. Therefore it can be used as a similarity measure. This information can also be combined with the orientation tensor to yield a rotation invariant similarity. As the orientation tensor uses the square of the similarity values, some pattern like lefthanded and righthanded rotation in 2D, or divergence and convergence, are not distinguished anymore. Furthermore, it does not work for arbitrary templates. Heiberg et al. [HEWK03] define no Fourier transform for their vector fields. However, treating the components of the vectors separately concerning Fourier transforms will work though it is mathematically unsatisfying.

Yet another approach for template matching of vector fields makes use of Clifford Algebra [ES03]. Clifford algebra [Hes86] extends the classical description of an Euclidean n-space as a real n-dimensional vector space with scalar product to a real algebra. In 3D, it has the basis $1, e_1, e_2, e_3, e_1e_2, e_2e_3, e_3e_1, e_1e_2e_3$. The elements of the algebra are called multivectors. The multiplication of multivectors is defined as associative, bilinear and by the equations

$$1e_j = e_j, \qquad j = 1,2,3$$

$$e_je_j = 1, \qquad j = 1,2,3$$

$$e_je_k = -e_ke_j, \qquad j,k = 1,2,3,\ j \neq k$$

Thus, a multiplication of vectors is described, too. The usual vectors $(x,y,z) \in \mathbb{R}^3$ are identified with

$$xe_1 + ye_2 + ze_3 \in E^3 \subset G^3.$$

The Clifford multiplication of two vectors $a, b \in E^3$ results in

$$ab = < a,b > + a \wedge b,$$

where $<,>$ is the inner product and $\wedge$ the outer product, and both can be extracted out of the multiplication result by a simple projection. Thus, the product of two vectors describes the rotation and scaling necessary to transform one vector into the other. Using this Clifford algebra, Clifford convolution [ES03] of two multivector valued fields **f** and **h** is defined as

$$(h * f)(x) = \int_{\mathbb{R}^d} h(x') f(x - x') |dx'|.$$

Note that a correlation can be computed via a convolution by adapting the template. Furthermore, this convolution gives an approximation of the relative geometric position of the structures in field and template allowing for rotation invariant template matching [ES03]. The direction of the structure can be computed out of the convolution. The template is then rotated in this direction and another convolution is computed for an orientation invariant similarity value. In this last step, only the scalar product is used as similarity value analog to the approach of Heiberg. When template and structure are equal and γ is removed from the result, then the similarity is 1.

In the convolution the approximations for the angle are summed and thus they can erase each other. Therefore it is not enough to compute one Clifford convolution for the approximation of the direction of the structure. Additional templates with different directions have to be used to overcome this problem. In [ES03], 3 template directions in 2D and 6 directions in 3D are used in order to get a stable and robust template matching algorithm.

The Clifford convolution is superior to the approach of Heiberg et al. since it provides a unified notation for convolution of scalar, vector and multivector fields. Furthermore, a corresponding Fourier transform has been developed for 2D and 3D vector fields and can be used for an acceleration of the convolution operations in the matching [ES05b]. The Clifford convolution is an extension of scalar field convolution from image processing and scalar convolution over vector fields defined by Heiberg et al. [HEWK03] and is used in the segmentation algorithm in this paper.

3. Segmentation

Before starting a segmentation, it has to be determined which features are of interest, and should form the template set. This includes specifying the type of feature like vortex, shear, sink, saddle or source (Figure 1) as well as the strength and size of the features and the scale at which they appear.

3.1. Challenges

The basic idea of segmenting a data set via template matching is quite easy: Determine all features present in the data set, compute their size and shape, and label all positions within the feature as belonging to it. All positions not labeled at all will be background, or not interesting at the moment. However, there are several challenges when trying to use this approach on vector fields.

3.1.1. Irregular Grids

Convolution and correlation are usually evaluated on uniform grids. However, many flow data sets are defined on irregular grids. There are several ways to deal with that. First of all, convolution can be transfered to irregular grids using resampling [ES05a]. However, the results depend on the resampling method used, and the convolution computation is slow. Therefore a resampling of the whole data set to a uniform grid is advised, and using a power of 2 for the number of grid points of each direction. Thus, the convolution theorem and fast Fourier transform algorithms can be applied for speeding up the convolution computations [ES05b].

3.1.2. Similarity Value

The similarity of two vector valued templates with respect to a direction is defined by the sum of the scalar product of their vectors. The similarity value itself depends on the magnitude of both the pattern in the field and the template itself. Therefore, the obtained similarity values are usually

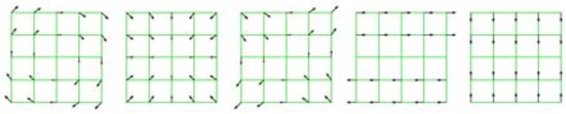

Figure 1: *A 2d template set. From left to right: rotation, convergence, saddle, shear flow, convergence line. Note that counterclockwise and divergence pattern can be found with these templates as well.*

scaled by the magnitude of the template:

$$s(x) = \frac{\langle h * f \rangle(x)}{\sum_{x' \in h} |h(x')|}$$

Often, this similarity is influenced more by the velocity magnitude of the vectors than their orientations. For a similarity measure which is independent of the velocity magnitude, the length of every vector in the field can be artificially set to one. This will be called normalization of the data set in this paper. Matching on a normalized data set corresponds to a matching of the streamlines rather than the vectors themselves. It is often used to enhance weak features.

Normalization of the data set will work very well in some cased, but not when the features are hidden by other components of the flow. Furthermore, normalization will shift the position of features, though only within cells, and can drastically change the size of features. When the velocity of vectors in the feature is important, for example in a Vatistas vortex [Vat98], normalization should not be used at all.

3.1.3. Position, Size and Scale

Scale space considerations should not be neglected within the segmentation. The size of the features, and thus the scales at which they appear and dissappear, can play an important role for the segmentation (Figure 2). The classification of the features, and thus the segmentation, can be done for each scale separately and be combined with scale space visualizations like Gaussian pyramids [Jai89,Jäh02]. Another possibility is to match each template using different template sizes. The resulting similarity images can then be combined into one scale invariant similarity image by using the maxima of the values at each position.

A scale-invariant similarity will also ensure a scale-invariant detection of the position of a feature as these are usually detected by local maxima of the magnitude of the similarity values. Note that the position of a feature would otherwise depend on the scale at which the feature is evaluated, e.g the center of a vortex with an elliptical shape will have different positions for different scales. Furthermore, the scale and template size resulting in the maximal similarity also gives size information of the feature. Though subpixel-accuracy is possible [ESvdW05], the authors propose to start with a template of size 3Δ for each direction where Δ is the (uniform) edge length. Then continue with all uneven template sizes as this will result in a growth of the radius of Δ.

The computation of the convolutions with different template sizes can be accelerated by computing the convolutions in Fourier domain [ES05b]. Another possibility is to start with a small template size and only compute similarities with larger templates where the similarities with the small template were above a certain threshold. The results depend on the choice of the threshold, and large features may be missed because they are hidden at the small scale. Furthermore, it also depends on the template itself. While this approach seems to be stable for e.g. rotational pattern, the similarities obtained for shear like pattern were often to small. However, this approach can give fast and useful results, especially for a first overall view of the data set.

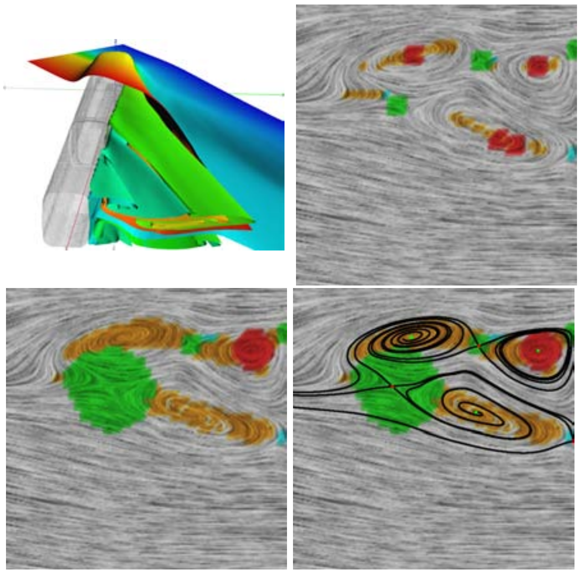

Figure 2: *Vortices generated by an ICE train (top left). Segmentation of a section plane through the flow (threshold=0.5), overlaid with LIC. The data set was normalized. Red: rotation, orange: shear flow, light blue: convergent/divergent line, green: saddle point. Top right: only 3x3 templates were used to determine the line features shear flow and convergent/divergent lines. Bottom: templates from size 3x3 till no significant similarities were gained were used to detect the features. Bottom right: Topology added. Note that the elliptical vortices are classified as shear flow when using larger templates.*

The size of a feature in flow field is usually hard to define. Point based features, like saddle points, usually have no size, and are visualized using only very small area. However, for segmentation and visualization issues, larger areas are preferred as they are not easily overlooked. The region around a point or line based feature classifies this feature, and therefore can be regarded as belonging to it. This is also the size that is computed by the approach above.

The size of a line based feature, e.g. a 2D shear flow, can be the length of the line, or the scale at which they appear. Due to the smoothing effect of template matching, the region with similarity values above a threshold will be larger for larger features. Thus, segmenting and visualizing thresholded similarities is often good enough in this case.

For region based features, the size of a feature model can be infinite, as e.g. in the Vatistas vortex model [Vat98]. However, the size of the vortex core region is an important information there. Again, this is exactly the size information given by scale invariant template matching.

3.1.4. Non-Orthogonal Feature Definitions

Some features are orthogonal to each other, that is their description and subsequent matching will not respond to the other features at all. One example of an orthogonal feature pair is pure rotation and pure convergence. Here, the classification of the features based on template matching and subsequent segmentation is obvious. But feature definitions can also overlap, for example a rotation and a shear flow both describe part of the phenomena of the other feature. Other pairs of features which describe similar phenomena are sinks and convergence lines, and sources and divergence lines. In these cases, more than the similarity of one template to the flow is non-zero at this position. Therefore the different similarity values have to be compared, and the feature classified according to the largest similarity value which has been computed. This also means that misclassification can take place. For example, an elliptical rotation can be more similar to the shear flow description than to a circular rotation (Figure 2), though it surely is a vortex. Using vector valued templates for the feature definition, orthogonality of features can easily be computed and quantified by correlation of the different templates: A pair of templates is orthogonal if, and only if, their (rotation invariant) similarity is zero.

3.1.5. Overlapping Features

There are also other reasons why more than one template will respond to the flow at a position. Convolution with a template is a linear operation. The linearity property is also known as the superposition principle. It means that complex flow can be analyzed by matching with several quite simple templates where the similarity values will indicate how much one template resembles the flow. It also indicates how much of the flow at this position is due to this particular feature model, and how much has to be described by other templates. An example is a swirling vortex which is a superposition of a perfectly circular rotation and a divergent flow (Figure 3). Another example is a wind tunnel, where the overall velocity of the air flow will usually hide smaller vortices [ESvdW05]. But this means that there may be more than one feature at a position, depending on whether this point of view is taken. In this case, segmentation is more challenging.

One solution is to classify the flow according to the most dominant feature at this position. But this is short-sighted as e.g. in the wind tunnel experiment only the overall flow will remain. Regarding the swirling vortex, one could classify it into a new class of swirling features. These swirling flows are then detected by using the already computed similarities to rotation and divergence templates. The percentage of these two similarities also gives a measure of the skewness of the swirl.

The issue of superposition and overlapping features leads to the proposition of computing a classification of the flow at every position into all of the features found there and the percentage in which they contribute to the flow. This is also a kind of segmentation, but one of the flow at one position into each of the interesting features. Note that when the data set has been normalized beforehand, the similarity values equal this percentage. Otherwise, the similarity values have to be scaled by the energy of the flow to obtain this information.

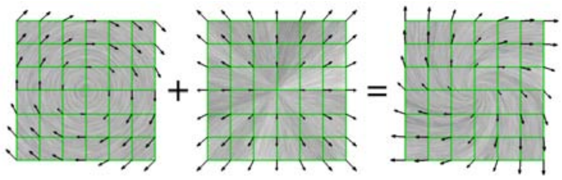

Figure 3: *Superposition of a rotation and a divergence results in a spiral pattern.*

3.1.6. Choice of Thresholds

The choice of suitable thresholds depends on the properties of the data set to be analyzed, and different choices of the threshold gives different results [Jai89, Jäh02] (Figure 4). When the data set has been normalized, and no constant flow hides the features, the similarity s is between $-1 \leq s \leq 1$. The authors have found that a threshold of 0.5 for the magnitude of s is a robust choice for their data. When the data

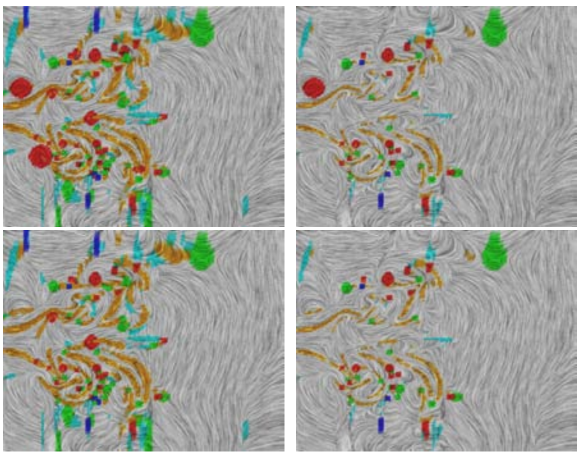

Figure 4: *A swirling jet data set. Segmentation and LIC. Red: rotation, orange: shear flow, light blue: convergent/divergent line, dark blue: sink/source, green:saddle. Left: threshold of 0.5, right: threshold of 0.7. Top: segmentation using the similarity values, bottom: when the difference between shear and rotation was below 0.05, the flow was classified as shear rather than rotation.*

has not been normalized, then $-\infty \leq s \leq \infty$. Then, a possible approach is to determine all similarities larger than one, or larger then a certain fraction of the maximal value determined by the algorithm. Generally, half the maximal computed similarity value is a valid choice.

3.2. The Algorithm

To summarize, the segmentation of vector fields is computed as follows:

1. Determination of the features of interest and the parameters to be computed
2. Grouping of the features for segmentation as well as visualization (e.g. all rotations, all shear flows, etc.)
3. Generation of (vector valued) templates describing the features or feature groups
4. For each feature:
   a. Template matching (rotational invariant) using different features sizes
   b. Thresholding of the resulting similarity values
   c. Computation of the maxima of the similarity values at each position, storing the corresponding feature sizes.
   d. Local maxima of the results determine position and size of the features
   e. Computation of possible other parameters of the features
5. For non-orthogonal features at one position, the features resulting in the smaller similarities are discarded
6. For orthogonal features at one position, the dominant feature is determined but all features are stored

3.3. 2D, 3D and Time-Dependent Data Sets

The vector-valued convolution is defined for arbitrary nD data sets. However, the rotation invariant matching is only defined for 2D and 3D so far. As 2D and 3D data sets are most common, the rotation invariant matching approach using Clifford convolution poses no disadvantages.

For time-dependent data sets, each time slice can be segmented separately and the resulting regions can be traced over time. Tracing algorithms are well known from image processing [Jai89, Jäh02], and can be applied directly as the similarity data is usually scalar valued. Furthermore, time dependent data is often visualized using movies which can be generated directly out of the single segmentations of the time-steps (Figure 5). Due to the averaging effect of the convolution, the similarity values are robust in terms of noise and small changes. This is beneficial for the tracking, and visual discontinuities over different time steps are not expected.

4. Results

The first data set used in this paper is a section plane through vortices generated by an ICE train (Figure 2). The train moves with a speed of 250 km/h. The wind comes directly from one side but due to the speed of the train, the angle of attack is 15 degree. A section plane through four of these vortices with dimensions 51×51 was computed. This data set was also included to remind of scale issues (Figure 2). Furthermore, it clearly shows the problem of classifying rotations and shear flow.

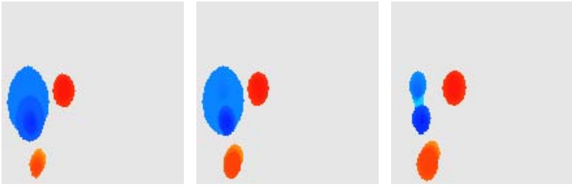

Figure 5: *Segmentations of three successive time steps of a swirling jet data set data set (from left to right, threshold=0.5). The data has been normalized before matching. Color coding: clockwise rotations in red and counterclockwise rotations in blue. From light to dark colors: increase in similarity values.*

The authors also studied data from CFD simulations describing a vortex breakdown, here swirling jets entering a fluid at rest (Figure 4 and 6). Vortex breakdown can be found in flows ranging from tornados, wing tip vortices, pipe flows to swirling jets. Here, the turbulent swirling jets enter a fluid at rest. The simulation considers a cylinder, so that a planar cut along the axis of the cylinder can be used as a domain. The domain is discretized by a 124×101 respectively. 251×159 rectilinear grid with smaller rectangles towards the axis of the cylinder. Since a lot of small and large scale vortices are present in the flow, a discrete numerical simulation (DNS) using a higher order finite difference scheme is used to solve the incompressible Navier-Stokes equations. The vector fields have been normalized before processing. The segmentation and subsequent visualization of the data sets highlights the features and thus guides the user through the data set. Some vortices are found in the data, and the layers of opposite flow, divided by shear flow, are clearly visible (Figure 4 and 6). The classification of the most dominant feature was challenging as the similarity values of matching e.g. shear and rotational templates at one position in the data set sometimes differed only by 0.0001, though both similarities were above the threshold. This usually indicates an elliptical vortex or a swirling motion generated by shear flow.

Another example of a swirling jet from CFD simulations are 125 timesteps of unsteady vorticity vector field of swirling jet on a 141×251 structured grid. The data was normalized and segmented into clockwise and counterclockwise rotations, and background. Three successive time steps are shown in Figure 5. In these timesteps, the split of a vortex into two new ones can be observed. The pairing of two vortices each of different rotation orientation, and the path of the moving vortices, can be easily studied using segmenta-

Figure 6: *Segmentation of a simulation of a swirling jet entering a fluid at rest (threshold=0.5). Red: rotation, orange: shear flow, light blue: convergent/divergent line, dark blue: sink/source, green: saddle. Top: whole data set. Middle and bottom left: zoomed in. Streamlines respectively. topology added. Bottom right: some details. Hedgehogs and streamlines added.*

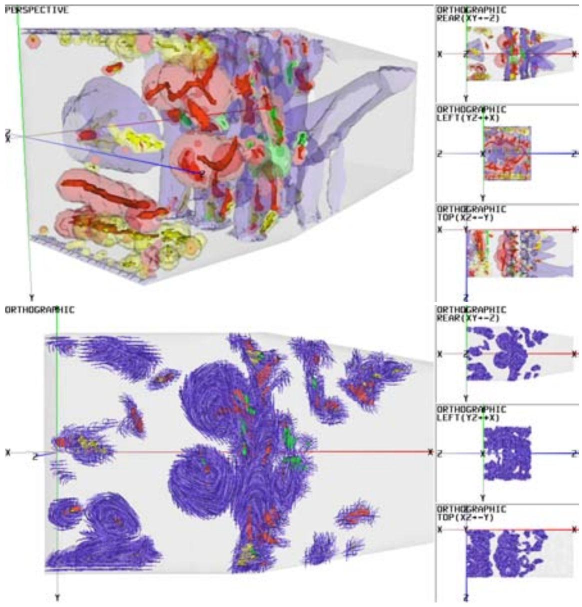

Figure 7: *Segmentation of the normalized gas furnace chamber (Threshold: 0.5). Isosurfaces of the results (Value 0.5): Red: rotations, yellow: shear flow, green: saddles. The cores of the regions are displayed, too, and in the same colors. Templates of divergence/convergence resulted in similarities below the threshold. Top: The velocity of the original data set is displayed at an isovalue of 15. Bottom: The results of the segmentation can also be used for streamline seeding.*

tion throughout all timesteps. Only a part of the data sets of these time steps is shown as the rest was classified as background.

An interesting data set is a gas furnace chamber as it is used for heating a house. The simulation solves compressible Navier-Stokes equations using a turbulent model applied on a irregular grid consisting of 174341 tetrahedra with 32440 vertices. For computational issues, the data was resampled onto a uniform grid with dimensions $126 \times 65 \times 57$. In Figure 7, the swirling gas enters the chamber in the center of the left face while the air enters from 9 openings on the top and 9 openings on the bottom, so that the combustion takes place in the center area of the chamber. The products of the combustion leave the chamber on the right. The flow is highly turbulent and exhibits a lot of different scale vortices.

The structures in the flow can easily be identified by the segmentation. Note that the shear flow at the front bottom (in yellow) is a misclassification, it is actually an elliptical vortex. This is one reason why the vortex core itself (in red) extends into this area. Note also the saddle line behind these vortices (in green), it is clearly visible in the bottom image.

Additional information of the gas furnace chamber can be gained by displaying an isosurface of the velocity of the original data set (Figure 7, blue isosurface). Using this isosurface, the gas and air inflow streams are clearly visible. Note the vortices besides them, and how they follow the shape of adjacent air streams.

5. Conclusion

The authors have presented an algorithm for automatic computation of a feature-based segmentation of 2D, 3D, and time dependent vector fields. The segmentation is based on template matching, thus obtaining intuitive results and robustness in terms of noise. Furthermore, the template matching allows an unified approach for the detection of different features.

Several challenges on designing the algorithm like misclassification and superposition effects have been presented and discussed. Some results have been presented, and especially the classification problem will be studied further.

The visualizations of the segmentations clearly depict the structures of the flow data as the features are displayed in conjunction with each other. Thus, even highly turbulent data can be studied easily.

6. Acknowledgments

We thank Prof. Kollmann, MAE department, University of California at Davis, for producing the swirling jet data sets and Markus Rütten, DLR Göttingen, for the ICE and the gas furnace chamber data set.

Furthermore, we like to thank the members of the FAnToM development team at the Technical University of Kaiserslautern, and University of Leipzig for their help with programming and production of the pictures.

References

[CL93] CABRAL B., LEEDOM L. C.: Imaging vector fields using line integral convolution. In *Proceedings of SIGGRAPH '93* (New York, 1993), pp. 263–270.

[DGH03] DOLEISCH H., GASSER M., HAUSER H.: Interactive feature specification for focus+context visualization of complex simulation data. In *Proceedings of the 5th Joint IEEE TCVG - EUROGRAPHICS Symposium on Visualization (VisSym 2003)* (Grenoble, France, 2003), pp. 239–248.

[DPR00] DIEWALD U., PREUSSER T., RUMPF M.: Anisotropic diffusion in vector field visualization on euclidean domains and surfaces. *IEEE Transactions on Visualization and Computer Graphics 6*, 2 (2000), 139–149.

[ES03] EBLING J., SCHEUERMANN G.: Clifford convolution and pattern matching on vector fields. In *Proceedings of IEEE Visualization 2003* (Los Alamitos, CA, 2003), IEEE Computer Society, pp. 193–200.

[ES05a] EBLING J., SCHEUERMANN G.: Clifford convolution and pattern matching on irregular grids. In *Scientific Visualization: The Visual Extraction of Knowledge from Data* (Berlin, Germany, 2005), Bonneau G., Ertl T.,, Nielson G., (Eds.), Springer.

[ES05b] EBLING J., SCHEUERMANN G.: Fourier transform on multivector fields. *IEEE Transactions on Visualization and Computer Graphics 11*, 4 (2005), 469–479.

[ESvdW05] EBLING J., SCHEUERMANN G., VAN DER WALL B.: Analysis and visualization of 3-c piv images from HART II using image processing methods. In *Data Visualization 2005* (2005), pp. 161–168.

[GK95] GRANLUND G. H., KNUTSSON H.: *Signal Processing For Computer Vision*. Kluwer Academic Publishers, 1995.

[GPR*04] GRIEBEL M., PREUSSER T., RUMPF M., SCHWEITZER A., TELEA A.: Flow field clustering via algebraic multigrid. In *Proceedings Visualization Conference 2004* (2004), IEEE CS Press.

[Hes86] HESTENES D.: *New Foundations For Classical Mechanics*. Kluwer Academic Publishers, Dordrecht, The Netherlands, 1986.

[HEWK03] HEIBERG E. B., EBBERS T., WIGSTRÖM L., KARLSSON M.: Three dimensional flow characterization using vector pattern matching. *IEEE Transactions on Visualization and Computer Graphics 9*, 3 (2003), 313–319.

[HH91] HELMAN J., HESSELINK L.: Visualizing vector field topology in fluid flows. *IEEE Computer Graphics and Applications* (1991), 36–46.

[Jäh02] JÄHNE B.: *Digitale Bildverarbeitung*. Springer Verlag, Berlin, Germany, 2002.

[Jai89] JAIN A. K.: *Fundamentals Of Digital Image Processing*. Prentice Hall, Englewoods Cliffs, NJ, USA, 1989.

[KHL99] KENWRIGHT D. N., HENZE C., LEVIT C.: Feature extraction of separation and attatchment lines. *IEEE Transactions on Visualization and Computer Graphics 5*, 2 (1999), 151–158.

[PP00] POLTHIER K., PREUSS E.: Variational approach to vector field decomposition. In *Eurographis Workshop on Scientific Visualization* (2000), Liere R., et al. F. P., (Eds.), pp. 113–134.

[PP03] POLTHIER K., PREUSS E.: Identifying vector field singularities using a discrete hodge decomposition. *Visualization and Mathematics III* (2003), 775–792.

[PVH*03] POST F. H., VROLIJK B., HAUSER H., LARAMEE R. S., DOLEITSCH H.: The state of the art in flow visualization: Feature extraction and tracking. *Computer Graphics Forum 22*, 4 (2003), 775–792.

[Rot00] ROTH M.: *Automatic Extraction Of Vortex Core Lines And Other Line Type Features For Scientific Visualization.* PhD thesis, ETH, 2000.

[TLHD03] TONG Y., LOMBEYDA S., HIRANI A., DESBRUN M.: Discrete multiscale vector field decomposition. *ACM Transactions on Graphics 22*, 3 (2003), 445–452.

[Tri02] TRICOCHE X.: *Vector and Tensor Field Topology Simplification, Tracking, and Visualization*. PhD thesis, University of Kaiserslautern, Germany, 2002.

[Vat98] VATISTAS G.: New model for intense self-similar vortices. *Experiments in Fluids 14*, 4 (1998), 462–469.

[vdWBY*04] VAN DER WALL B. G., BURLEY C. L., YU Y. H., RICHARD H., PENGEL K., BEAUMIER P.: The HART II test - measurement of helicopter rotor wakes. *Aerospace Science and Technology 8*, 4 (2004), 273–284.